

# Quantum simulation of Fenna-Matthew-Olson(FMO) complex on a nuclear magnetic resonance(NMR) quantum computer

M. Mahdian<sup>\*1</sup>, H. Davoodi Yeganeh<sup>†1</sup>, and A. Dehghani<sup>‡2</sup>

<sup>1</sup>Faculty of Physics, Theoretical and astrophysics department ,  
University of Tabriz, 51665-163 Tabriz, Iran

<sup>2</sup>Department of Physics, Payame Noor University, P. O. Box  
19395-3697, Tehran, Iran

April 9, 2019

## Abstract

Dynamical simulation of light-harvesting complexes as open quantum systems, in the weak and strong coupling regimes, has been recently attended. In this paper, we investigate a digital approach to quantum and dynamical simulation of a photosynthetic FMO complex surrounded with a Markovian bath, i.e., memoryless, with a nuclear and spin-based quantum simulator. For this purpose, we apply the re(de)coupling method on a nuclear magnetic resonance (NMR) quantum computation and Solovay-Kitaev decomposition technique for single-qubit channels. Finally, we use the near-term quantum computer that developed by Rigetti to implement circuits. As a result we show an efficient quantum simulation of a photosynthetic system.

---

<sup>\*</sup>mahdian@tabrizu.ac.ir

<sup>†</sup>h.yeganeh@tabrizu.ac.ir

<sup>‡</sup>adehghani@pnu.ac.ir

**Keywords** Quantum simulation, FMO complex, Nuclear spin systems, NMR quantum computation.

## 1 Introduction

Understanding the quantum dynamics of an interacting system including many degrees of freedom in an environment is one of the big challenges in physics, chemistry and biology. Due to the exponential growth of variables, classical computational methods fail to simulate quantum systems with complex many-body interactions. For this reason, the idea of modeling a quantum computer to simulate large quantum systems was originally suggested by R. Feynman [1], where he conjectured that the quantum computers might be able to carry the simulation more efficiently than the classical one. Although, implementation of universal quantum computers for a large size of open quantum systems are not available yet. According to this, a quantum simulation was proposed to solve such an exponential explosion problem using a controllable quantum system [1], and typically classified into two main categories, namely, the analog and digital one. The analog quantum simulator is a device that uses to mimic quantum bits map onto qubits, modes onto modes and so on while this approach is not universal. However, the digital quantum simulators allow us to reproduce quantum dynamics that are difficult with analog quantum simulators by a universal digital decomposition of its Hamiltonian into efficient elementary gates. Also, different platforms have been used for implementing quantum simulators, such as ions trapped in the optical cavity [2, 3], cold atoms in optical lattices [4], superconducting qubits [5, 6], photons [7], quantum dots [8] and the spin qubits based on magnetic resonance process [9, 10, 11, 12, 13].

During last decades the dynamical evolution of closed and, especially, open quantum systems have been attracted great interests. It is well known that the dynamical behavior of a closed system can be described by a unitary transformation, which can be simulated directly with a quantum simulator. However, in a real world all quantum systems are invariably connected with their environment. Such systems are called, usually, as open quantum systems, and their dynamical treatment due to the decoherence and dissipation effects isn't unitary. It is worth mentioning that the quantum dynamics of an open quantum system is very complex and often used to describe the dynamics of proximity like the Born-Markov approximation [14]. Because

of this, a lot of analytical and numerical methods had, also, been employed to simulate the dynamics of open quantum systems [15, 16, 17, 18, 19, 20]. We will consider quantum dynamics of photosynthetic light-harvesting complexes that are the main sources of energy for plant's algae and some kinds of bacteria. In all of the photosynthetic organisms, light is absorbed by pigments such as chlorophyll and carotene in antenna complexes, and then this energy transfers as an electronic excitation to a reaction center where charge separation occurs through the Fenna-Matthew-Olson (FMO) complex. The FMO complex is made of three identical monomers where each monomer involves seven bacteriochlorophyll molecules surrounded by a protein environment. So it can be modeled by a system of seven qubits. Neill Lambert et al. [21] introduced an interesting progress in quantum biology, where they performed an experimental and theoretical studies on the photosynthesis such as the quantum coherent energy transport, entanglement and tests of quantumness. De-coherence in biological systems is being studied in Ref. [22] and principles of a noise-assisted transport as well as the origin of long-lived coherences for the FMO complex in photosynthesis was given. The exciton-energy transfer in light-harvesting complexes has been investigated by various methods such as the Forster theory in a weak molecular interaction limit or by the Redfield master equations derived from Markov approximation in a weak coupling regime between molecules and environment [23, 24, 25, 26, 27, 28]. In general, non-Markovian effects on energy transfer dynamic are significant [29, 30]. Here we ignore the non-Markovian effects on energy-transfer dynamics and consider the FMO complex in a Markovian regime. It should be noticed that an effective dynamics of the FMO complex is modeled by a Hamiltonian which describes the coherent exchange of excitations among different sites, also local Lindblad terms that takes into account the dissipation and dephasing processes caused by a surrounding environment [31].

In the one hand, dynamical simulations of the light-harvesting complexes have considered and a large number of various experimental and analytical studies have been done. For instance, numerical analysis of a spectral density based on the molecular dynamics has been studied in Refs. [30, 32], as well as the corresponding dynamics had been investigated based on a two-dimensional electronic spectroscopy [33], super-conducting qubits [34] and numerically simulations [35]. On the other hand, nuclear spin systems are good candidates for a quantum simulator, because they include long coherence times and may be manipulated by complex sequences of radio frequency

(RF) pulses, then they can be carried out easily using modern spectrometers. Because of the importance of the subject, we present an effective nuclear spin systems using a NMR-based quantum simulator as a controllable quantum system which can be applied to simulate the dynamics of FMO complex. We investigate a scheme based on the recoupling and decoupling methods [36] which are particularly relevant to the connection of any two nuclear spins using RF pulses in any selected time for simulating of the Hamiltonian of FMO complex. Here, we assume the Solovay-Kitaev decomposition strategy for single-qubit channels [20] to simulate the non-unitary part of quantum master equation and circuits obtained on the NMR quantum computation.

The paper is organized as follows. In Sec. 2, FMO complex will be introduced. In Sec. 3, simulation of Hamiltonian of the FMO complex by a NMR simulator are expressed. In Sec. 4, corresponding calculations to simulate the non-unitary part will be given. Finally, Sec. 5 is devoted to some conclusions.

## 2 FMO complex

The FMO complex is generally constituted of multiple chromophores which transform photons into exactions and transport photons to a reaction center. As mentioned above, an efficient dynamics of the FMO complex can be expressed by a composite spin Hamiltonian, which contains the coherent exchange of excitation and local Lindblad terms [31], as follows:

$$H = \sum_{j=1}^7 \epsilon_j \sigma_j^+ \sigma_j^- + \sum_{j \neq l}^7 \hbar \nu_{jl} (\sigma_j^+ \sigma_l^- + \sigma_j^- \sigma_l^+), \quad (1)$$

where  $\sigma_j^+$  ( $\sigma_j^-$ ) is raising (lowering) operator for  $j^{\text{th}}$  site,  $\epsilon_j$  is the corresponding energy and  $\nu_{jl}$  is the hopping rate of excitation between the  $j^{\text{th}}$  and  $l^{\text{th}}$  sites. Along with considering  $\sigma_j^{\pm} = \sigma_j^x \pm \sigma_j^y$  and putting  $\hbar = 1$ ,  $t$  can be decomposed into a single-qubit Hamiltonian  $H_0$  and an interaction Hamiltonian  $H_I$ , i.e.

$$H = \underbrace{\sum_{j=1}^7 \epsilon_j \sigma_j^z}_{H_0} + \underbrace{\sum_{j \neq l}^7 \nu_{jl} (\sigma_j^x \sigma_l^x + \sigma_j^y \sigma_l^y)}_{H_I}. \quad (2)$$

For expressing the dynamics of non-unitary part,  $H_I$  we assume that the system affected by two distinct types of noise are called the dissipative and

dephasing processes. Dissipative effect passes the excitation energy with rate  $\Gamma_j$  to an environment and dephasing process destroys the phase coherence with rate  $\gamma_j$  of the site  $j^{th}$ . Both of these can be regarded in the Markovian master equation with local dephasing and dissipation terms. For the FMO complex in the Markovian master equation approach, the dissipative and the dephasing processes are captured, respectively, by the Lindblad super-operators as follows

$$\mathcal{L}_{diss}(\rho) = \sum_{j=1}^7 \Gamma_j (-\sigma_j^+ \sigma_j^- \rho - \rho \sigma_j^+ \sigma_j^- + 2\sigma_j^- \rho \sigma_j^+), \quad (3)$$

$$\mathcal{L}_{deph}(\rho) = \sum_{j=1}^7 \gamma_j (-\sigma_j^+ \sigma_j^- \rho - \rho \sigma_j^+ \sigma_j^- + 2\sigma_j^+ \sigma_j^- \rho \sigma_j^+ \sigma_j^-). \quad (4)$$

Finally, the total transfer of excitation is measured by the population in the sink. In the next section we introduce recoupling and decoupling method attached to simulate the Hamiltonian of the FMO complex.

### 3 Simulation of Hamiltonian of the FMO complex with recoupling and decoupling method

We use, here, recoupling and decoupling method with Hadamard matrix's approach to simulate the Hamiltonian of FMO complex, and perform a specific coupling in the NMR quantum computation. The task of turning-off all the couplings is known as decoupling, and also doing this for a selected subset of couplings is known as recoupling. These pulses are single-qubit operations that transfer Hamiltonian in time between two pulses so that un-wanted couplings in a consecutive evolution cancel each other [36]. Decoupling part must be chosen as the Hadamard matrices  $H(n)$ , where we have used  $\pm 1$  instead of the positive and negative sign, respectively. So the matrix  $S_n$  will be achieved, where each column represents a time interval ( $U$ ) and each row indicates a qubit. Everywhere exists minus sign before and after the time interval means that there's a pulse  $X \equiv \sigma^x$  has been applied. When  $H(n)$  does not necessarily exist, we start with  $H(n)$  and finally take  $S_n$ . Similarly, for the recoupling part we use a normalized Hadamard matrix  $H(\bar{n})$  which has only +'s in the first row and column. Then, to implement selective recoupling between the  $i^{th}$  and  $j^{th}$  qubit, we exclude the first row and taking

the second row of  $H(\bar{n})$  to be the  $i^{th}$  and  $j^{th}$  qubit row of  $S_n$ , also the other  $n - 2$  rows of  $S_n$  can be chosen from the remaining rows of  $H(\bar{n})$ . Now we are in a position to simulate the Hamiltonian of the FMO complex:

$$H_{sim} \equiv H_{NMR} = \sum_{l=1}^N \frac{1}{2} \omega_l \sigma_l^z + \sum_{l=1}^{N-1} J_l \sigma_l^z \sigma_{l+1}^z, \quad (5)$$

where  $H_{NMR}$  called Longitudinal Ising model in solid state systems, and  $J_l$  denotes a coupling strength between the  $l^{th}$  and  $(l + 1)^{th}$  qubits. This Hamiltonian evolved in time by the following unitary operator

$$U_{NMR} \equiv U(\tau) = e^{-i\frac{\tau}{4} H_{NMR}}. \quad (6)$$

To simulate the Hamiltonian of Eq.(2), at first, we will simulate  $H_0$  with recoupling, second simulate  $H_I$  with decoupling methods. Finally, using the Trotter's formula [37], leads to the time evolution of Hamiltonian was given in Eq. (1).

### 3.1 Simulation of Hamiltonian $H_0$

It is clear that the Hamiltonian of FMO complex includes seven-qubits, then the sign matrix should have seven rows. On the other hand, Hadamard matrix of order-7 does not exist, then we consider a Hadamard matrix of order-8 to obtain a sign matrix  $S_7$ . We obtain the time evolution for the first qubit and generalize it to seven qubits, for this purpose by using the Eq.(6), and removing the last row of  $H(8)$ :

$$H(8) = \begin{pmatrix} +1 & +1 & +1 & +1 & +1 & +1 & +1 & +1 \\ +1 & -1 & +1 & -1 & +1 & -1 & +1 & -1 \\ +1 & +1 & -1 & -1 & +1 & +1 & -1 & -1 \\ +1 & -1 & -1 & +1 & +1 & -1 & -1 & +1 \\ +1 & +1 & +1 & +1 & -1 & -1 & -1 & -1 \\ +1 & -1 & +1 & -1 & -1 & +1 & -1 & +1 \\ +1 & +1 & -1 & -1 & -1 & -1 & +1 & +1 \\ +1 & -1 & -1 & +1 & -1 & +1 & +1 & -1 \end{pmatrix}, \quad (7)$$

a possible sign matrix  $S_7$  can be obtained as follows

$$S_7 = \begin{pmatrix} + & + & + & + & + & + & + & + \\ + & - & + & - & + & - & + & - \\ + & + & - & - & + & + & - & - \\ + & - & - & + & + & - & - & + \\ + & + & + & + & - & - & - & - \\ + & - & + & - & - & + & - & + \\ + & + & - & - & - & - & + & + \end{pmatrix}. \quad (8)$$

In continuation with the following pulse sequence

$$U(\sigma_x^2 \sigma_x^4 \sigma_x^6 U \sigma_x^2 \sigma_x^4 \sigma_x^6)(\sigma_x^3 \sigma_x^4 \sigma_x^7 U \sigma_x^3 \sigma_x^4 \sigma_x^7)(\sigma_x^2 \sigma_x^3 \sigma_x^6 \sigma_x^7 U \sigma_x^2 \sigma_x^3 \sigma_x^6 \sigma_x^7) \\ (\sigma_x^5 \sigma_x^6 \sigma_x^7 U \sigma_x^5 \sigma_x^6 \sigma_x^7)(\sigma_x^2 \sigma_x^3 \sigma_x^5 U \sigma_x^2 \sigma_x^3 \sigma_x^5)(\sigma_x^2 \sigma_x^4 \sigma_x^5 \sigma_x^7 U \sigma_x^2 \sigma_x^4 \sigma_x^5 \sigma_x^7)(\sigma_x^3 \sigma_x^4 \sigma_x^5 \sigma_x^6 U \sigma_x^3 \sigma_x^4 \sigma_x^5 \sigma_x^6),$$

using the Eq.(6) and the Paul matrices, we have

$$\left[ e^{-i\frac{\tau}{4} H_{NMR}} \sigma_x^2 \sigma_x^3 \sigma_x^4 \sigma_x^5 \sigma_x^6 \sigma_x^7 e^{-i\frac{\tau}{4} H_{NMR}} \sigma_x^3 \sigma_x^5 \sigma_x^7 \right]^2, \quad (9)$$

which provides a time evolution of the first qubit, i.e.

$$u_1^z(\tau) = e^{-i\frac{\tau}{2} \omega_1 \sigma_1^z}. \quad (10)$$

Quantum circuits to simulate  $u_1^z(\tau)$  is shown in Figure 1. Similarly, for seven qubits it can be written as

$$e^{-iH_0 t} = \otimes_{l=1}^7 u_l^z(\tau). \quad (11)$$

with

$$u_l^z(\tau) = [e^{-i\frac{\tau}{4} H_{NMR}} T_l' e^{-i\frac{\tau}{4} H_{NMR}} T_l']^2, \quad (12)$$

where  $T_l' = \otimes_{j \neq l} \sigma_j^x$ ,  $T_l = \otimes_{j \neq l} \sigma_j^x$  with  $l = 1, 2, \dots, 6$ , and prime denotes that if  $j$  is odd (even) number,  $l$  is considered as a even (odd) number. Then, the time evolution of  $H_0$  obtain at  $\tau = 4t$ .

To test our quantum circuit, we use the Forest (pyQuil) software platform. It is an open-source Python library developed by Rigetti for constructing, analyzing, and running quantum programs [38]. We consider initial state as  $|0000000\rangle$ , and then putting  $\tau = 1$ , implement our circuit. The output of circuit on Forest is

$$(0.8775825619 - 0.4794255386j)|0000000\rangle,$$

which matches the theory, i.e. is equivalent to  $U_1^z(\tau)|0000000\rangle$ . Since the time evolution occurred only on the first qubit, it means that the recoupling has done( See Appendix I for details and some code).

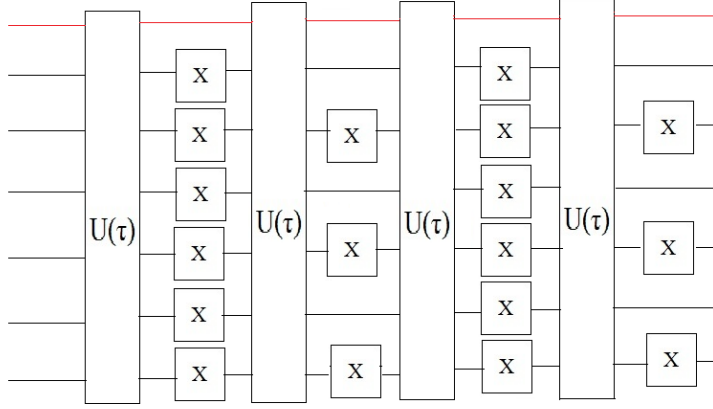


Figure 1: The quantum circuit to realize  $U_1^z(\tau)$  from  $U_{NMR} \equiv U(\tau)$ . Red line shows the first qubit in the system and  $X^i$  stand for gate  $\sigma_x^i$

### 3.2 Simulation of $H_I$

In this sub-section, we simulate a time evolution of the Hamiltonian  $H_I$ , by using a decoupling method. Similar to the case already discussed in previous section, the sign matrix  $S_7$  is obtained by a Hadamard matrix  $H(8)$ . We implement recoupling between the 3<sup>rd</sup> and 4<sup>th</sup> qubits and finally expressed in the general case for seven qubits. Firstly, we exclude the first row of  $H(8)$  and take the second row of  $H(8)$  to be the 3<sup>rd</sup> and 4<sup>th</sup> qubit row of  $S_7$ . Finally five other rows of  $S_7$  can be chosen from the remaining rows of  $H(8)$ . A possible structure is

$$S_7 = \begin{pmatrix} + & + & - & - & + & + & - & - \\ + & - & - & + & + & - & - & + \\ + & - & + & - & + & - & + & - \\ + & + & + & + & - & - & - & - \\ + & - & + & - & - & + & - & - \\ + & + & - & - & - & - & + & + \end{pmatrix}, \quad (13)$$

in this case the pulse sequence can be written as

$$U(\sigma_x^2 \sigma_x^3 \sigma_x^4 \sigma_x^6 U \sigma_x^2 \sigma_x^3 \sigma_x^4 \sigma_x^6) (\sigma_x^1 \sigma_x^2 \sigma_x^7 U \sigma_x^1 \sigma_x^2 \sigma_x^7) (\sigma_x^1 \sigma_x^3 \sigma_x^4 \sigma_x^7 U \sigma_x^1 \sigma_x^3 \sigma_x^4 \sigma_x^7) \\ (\sigma_x^5 \sigma_x^6 \sigma_x^7 U \sigma_x^5 \sigma_x^6 \sigma_x^7) (\sigma_x^2 \sigma_x^3 \sigma_x^4 \sigma_x^5 \sigma_x^7 U \sigma_x^2 \sigma_x^3 \sigma_x^4 \sigma_x^5 \sigma_x^7) (\sigma_x^1 \sigma_x^2 \sigma_x^5 \sigma_x^6 U \sigma_x^1 \sigma_x^2 \sigma_x^5 \sigma_x^6)$$



$$(\sigma_x^1 \sigma_x^3 \sigma_x^4 \sigma_x^5 \sigma_x^6 U \sigma_x^1 \sigma_x^3 \sigma_x^4 \sigma_x^5 \sigma_x^6).$$

Along with the identity  $\sigma_x^2 = I$ , it can be recast into:

$$e^{-i\tau J_3 \sigma_3^z \sigma_4^z} = U_{34}^{zz}(\tau) = U(\sigma_x^1 \sigma_x^2 \sigma_x^4 \sigma_x^5 \sigma_x^6 \sigma_x^7 U \sigma_x^1 \sigma_x^5 \sigma_x^7) U(\sigma_x^1 \sigma_x^2 \sigma_x^4 \sigma_x^5 \sigma_x^6 \sigma_x^7 U \sigma_x^1 \sigma_x^5 \sigma_x^7). \quad (14)$$

Note we consider  $x - x$  and  $y - y$  interaction for two nearest-neighbor-interacting qubits, and then by using the single-qubit operations, we obtain:

$$U_{34}^{xx+yy}(\tau) = e^{-i\tau H_{34}^{xy}} = e^{i\frac{\pi}{4} \sigma_3^y \sigma_4^y} U_{34}^{zz} e^{-i\frac{\pi}{4} \sigma_3^y \sigma_4^y} e^{i\frac{\pi}{4} \sigma_3^x \sigma_4^x} U_{34}^{zz} e^{-i\frac{\pi}{4} \sigma_3^x \sigma_4^x}, \quad (15)$$

where we have used the notation  $H_{34}^{xy} = J_3(\sigma_3^x \sigma_4^x + \sigma_3^y \sigma_4^y)$ . Also, for seven qubits it can be written, generally, as follows

$$U_{ll+1}^{xx+yy}(\tau) = e^{-i\tau H_{ll+1}^{xy}} = e^{i\frac{\pi}{4} \sigma_l^y \sigma_{l+1}^y} U_{ll+1}^{zz} e^{-i\frac{\pi}{4} \sigma_l^y \sigma_{l+1}^y} e^{i\frac{\pi}{4} \sigma_l^x \sigma_{l+1}^x} U_{ll+1}^{zz} e^{-i\frac{\pi}{4} \sigma_l^x \sigma_{l+1}^x},$$

where  $\tau = t$ ,  $J_l = 2\nu_{jl}$  with  $l = 1, 2, \dots, 6$  and considering  $H_l^{xy} = J_l(\sigma_l^x \sigma_{l+1}^x + \sigma_l^y \sigma_{l+1}^y)$ . Quantum circuits to simulate  $U_{34}^{xx+yy}(\tau)$  is shown in figure 2. Similar to the previous one, by implementing circuit on the Forest's software platform by:

$$\begin{aligned} & (0.0690086667 - 0.9957193521j)|00000000\rangle \\ & + (-0.0346499137 + 0.0177942584j)|00000100\rangle \\ & + (0.0273581824 - 0.0386110549j)|00001000\rangle \\ & + (-0.0034121934 + 0.0035492127j)|00001100\rangle, \end{aligned}$$

it is approximately equal with direct calculation of  $U_{34}^{xx+yy}(\tau)|00000000\rangle$ . It is easily seen that coupling between the 3<sup>th</sup> and 4<sup>th</sup> site is conserved, i.e. the decoupling yield with high efficiency. With all nearest-neighbor coupling operators  $U_{ll+1}^{zz}$  and  $U_{ll+1}^{xx+yy}$  being simulated, one can extend them to the long-range interactions in an straightforward manner. Since, both the Hamiltonian  $H_0$  and  $H_I$  are available, then the total Hamiltonian  $H$  can be obtained by the Trotters formula [37]:

$$e^{-iHt} = e^{-iH_0 t} e^{-iH_I t} + o(t^2). \quad (16)$$

Here we have used ( $H_{NMR}$ ) as a Hamiltonian simulator, which can be used instead of other Hamiltonian such as the transverse Ising model, the XY and Heisenberg model.

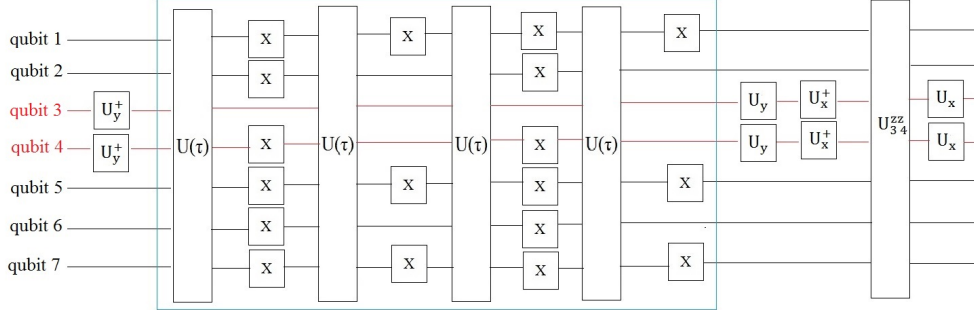


Figure 2: The quantum circuit is characterized the XY exchange interaction on the qubits third and fourth,  $U_{34}^{xx+yy}(\tau)$ . Rectangular boxes connecting to simulating  $U_{34}^{zz}(\tau)$  directly from  $U_{NMR} \equiv U(\tau)$

## 4 Quantum simulation of the non-unitary part dynamics

Clearly, it can be deduced from the non-unitary part of the FMO complex that each monomer has seven bacteria and considered as a system of seven qubits. We consider one of them which interacts with their surroundings and study its dynamics with the single-qubit channels approach. So we restrict ourselves to single-qubit states and begin by recalling some geometric properties of them [39]. In general, every density matrix  $\rho$  can be written in terms of the standard bases,  $\{I, \sigma^x, \sigma^y, \sigma^z\}$ , as  $\rho = \frac{1}{2}(I + \mathbf{r} \cdot \boldsymbol{\sigma})$  with  $\mathbf{r} \in \mathbb{R}^3$  and  $|\mathbf{r}|=1$ . Each single qubit quantum channel can then be represented in this basis by a unique  $4 \times 4$  matrix  $T = \begin{pmatrix} 1 & \mathbf{0} \\ \mathbf{m} & M \end{pmatrix}$ , where  $M$  is a  $3 \times 3$  matrix and  $\mathbf{0}$ ,  $\mathbf{m}$  denote row and column vectors respectively. The density matrix through the action of a channel will change as follows.

$$T(\rho) = \rho' = \frac{1}{2}(I + r' \cdot \boldsymbol{\sigma}), \quad (17)$$

with  $r' = M \cdot r + \mathbf{m}$  and the channel,  $T$ , is considered as an affine map, i.e.

$$T = \begin{pmatrix} 1 & 0 & 0 & 0 \\ 0 & \Lambda_1 & 0 & 0 \\ 0 & 0 & \Lambda_2 & 0 \\ m_3 & 0 & 0 & \Lambda_3 \end{pmatrix}, \quad (18)$$

by

$$M = \begin{pmatrix} \Lambda_1 & 0 & 0 \\ 0 & \Lambda_2 & 0 \\ 0 & 0 & \Lambda_3 \end{pmatrix}. \quad (19)$$

Also the matrix  $T$  can be rewritten in the following form

$$T = \begin{pmatrix} 1 & 0 & 0 & 0 \\ 0 & \cos v & 0 & 0 \\ 0 & 0 & \cos \mu & 0 \\ \sin v \sin \mu & 0 & 0 & \cos v \cos \mu \end{pmatrix}, \quad (20)$$

in this case, the Kraus operators will be given by

$$K_1 = \begin{pmatrix} \cos \beta & 0 \\ 0 & \cos \alpha \end{pmatrix}, \quad (21)$$

$$K_2 = \begin{pmatrix} 0 & \sin \alpha \\ \sin \beta & 0 \end{pmatrix}, \quad (22)$$

where  $\alpha = \frac{1}{2}(\mu + v)$  and  $\beta = \frac{1}{2}(\mu - v)$ . For one qubit state the Eq. (3) becomes

$$\mathcal{L}_{diss}(\rho) = \Gamma(-\sigma^+ \sigma^- \rho - \rho \sigma^+ \sigma^- + 2\sigma^- \rho \sigma^+), \quad (23)$$

by using the damping basis methods [40, 41] (details are given in the Appendix) and considering

$$\Lambda_{1,2} = e^{-4\Gamma t}, \Lambda_3 = e^{-8\Gamma t}, m_3 = e^{-8\Gamma t} - 1,$$

one can find  $\rho'$  as the following equation

$$\rho' = \frac{I + (-1 + e^{-8\Gamma t}(1 + r_z))\sigma_z + r_x \sigma_x e^{-4\Gamma t} + r_y \sigma_y e^{-4\Gamma t}}{2}. \quad (24)$$

Any single-qubit channel  $T$  (CPTP map) can be simulated with one ancillary qubit, one CNOT and four single-qubit operations[20]. The two rotation operations are applied to cover the Kraus operators action, and another single-qubit operation is used only to diagonalize the matrix  $M$ . We want to design a circuit to simulate the non-unitary part dynamics of the FMO complex on NMR computer. So recalling some properties of the NMR quantum computation [42], we shall consider a physical system which consists of a solution of identical molecules. Each molecule has  $N$  magnetically inequivalent nuclear spins, which serve as qubits. Nuclear spins interact via

dipole-dipole coupling or indirect coupling mediated by electrons. In any case, in the presence of a strong external magnetic field, only the secular parts are important [36]. Single qubit operations can be induced by the RF magnetic fields, oriented in the  $x - y$  plane perpendicular to the static field. The RF pulse can be selectively addressed spin  $i$  by an oscillator at angular frequency  $\omega_i$ . The general form of single-qubit gates in quantum information processing may become as the RF pulse along the  $\hat{n}$ -axis induces the rotation operator  $e^{-i\frac{t_{pw}}{2}\sigma \cdot \hat{n}}$  where  $t_{pw}$  is proportional to the pulse duration (pulse width) and amplitude. For example  $X = ie^{-i\frac{\pi}{2}\sigma_x}$  can be considered as a single  $\pi$ - pulse around  $\hat{x}$ -axes, then the Hadamard gate  $H = ie^{-i\frac{\pi}{2}\sigma_x}e^{-i\frac{\pi}{2}\sigma_y}$  can create a  $\frac{\pi}{2}$ -pulse around  $\hat{y}$ -axes followed by a  $\pi$ -pulse around  $\hat{x}$ -axes, too. Coupled logic gates can be naturally performed by a time evolution of the system. It can be assumed that the individual coupling term can be selectively turned on to perform a coupled operation between  $i^{th}$  and  $j^{th}$  qubits, next turning on the coupling term  $g_{ij}\sigma_z^i \otimes \sigma_z^j$  for time  $t$ , leads to the evolution or logic gate  $e^{-itg_{ij}\sigma_z^i \otimes \sigma_z^j}$ . Together with setting all of single-qubit transformations, the  $CNOT_{ij} = (I_i \otimes H_j)Cz(I_i \otimes H_j)$  fulfill a requirement for universality. Returning to the original problem and starting by the following assumptions:

$$\cos \alpha = e^{-4\Gamma t}, \quad \cos \beta = 1, \quad \sin \alpha = \sqrt{1 - e^{-8\Gamma t}}, \quad \sin \beta = 0,$$

the kraus operators are obtained as follows

$$K_1^{diss} = \begin{pmatrix} 1 & 0 \\ 0 & e^{-4\Gamma t} \end{pmatrix}, \quad (25)$$

$$K_2^{diss} = \begin{pmatrix} 0 & \sqrt{1 - e^{-8\Gamma t}} \\ 0 & 0 \end{pmatrix}. \quad (26)$$

As mentioned above an action of the Kraus operators can be represented through the rotations  $R_y(2\delta_1(2)) = e^{-i\sigma_y\gamma_1(2)}$  with  $2\delta_1 = \beta - \alpha + \frac{\pi}{2}$  and  $2\delta_2 = \beta + \alpha - \frac{\pi}{2}$  in a quantum circuit. For implementing the rotations  $R_y(2\delta_1)$  and  $R_y(2\delta_2)$ , respectively, we set

$$t_{pw} = 2\delta_1 = -Arc \cos(-4\Gamma t) + \frac{\pi}{2} \quad \text{and} \quad \hat{n} = \hat{y}, \quad (27)$$

and

$$t_{pw} = 2\delta_2 = Arc \cos(-4\Gamma t) - \frac{\pi}{2} \quad \text{and} \quad \hat{n} = \hat{y}. \quad (28)$$

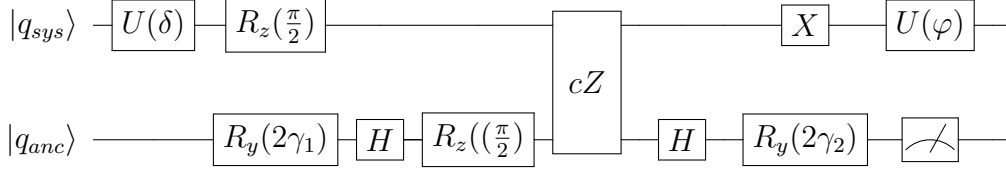


Figure 3: The quantum circuit to implement the simulation of one qubit dynamics on **the** nuclear spin system. The unitary operators  $U(\delta)$  and  $U(\phi)$  serve diagonalize the channel and  $|q_{sys}\rangle$ ,  $|q_{anc}\rangle$  denote **the** state of system and ancilla qubit respectively.

Along with the CNOT gate and above mentioned preliminaries we can obtain a quantum circuit for implementation of quantum channel of T for dissipation process that shown in Figure. 3. For dephasing process, a straightforward calculations of the Kraus operators leads to

$$K_1^{deph} = \begin{pmatrix} \frac{-1}{2}e^{-2\gamma t} & 0 \\ 0 & \frac{1}{2}e^{-2\gamma t} \end{pmatrix}, \quad (29)$$

$$K_2^{deph} = \begin{pmatrix} 0 & \sqrt{1 - \frac{1}{2}e^{-2\gamma t}} \\ \sqrt{1 - \frac{1}{2}e^{-2\gamma t}} & 0 \end{pmatrix}, \quad (30)$$

similarly, this process is also implemented based on the NMR simulator. In comparing with implementation process of the  $R_y(2\gamma_1)$  and  $R_y(2\gamma)$  we choose here  $t_{pw} = 2\gamma_1 = [\text{Arc cos}(-\frac{e^{-2\gamma t}}{2})]/2$  and  $\hat{n} = \hat{y}$  and  $t_{pw} = 2\gamma_2 = -\frac{\pi}{2}$  and  $\hat{n} = \hat{y}$  respectively.

## 5 Conclusion

In this paper, we investigated **a** quantum simulation of the FMO complex dynamics by nuclear spin systems. We employed recoupling and decoupling methods to simulate the Hamiltonian of FMO complex, then for quantum simulation of the non-unitary part dynamics of FMO complex with single-qubit channel's a quantum circuit had obtained. Finally, the obtained circuit implements a NMR quantum computation based on the Forest's software platform (pyQuil). The output of pyQuil code is compatible by direct calculation, too. Also, dynamical simulation of the FMO complex optimized with currently available technology. However, we will study non-Markovian dynamics of the FMO complex base on NMR quantum computation in the

future.

### Appendix I

As mentioned above pyQuil is an open-source Python library developed by Rigetti for constructing, analyzing, and running quantum programs. It is built on top of Quil, an open quantum instruction language (or simply quantum language), designed specifically for near-term quantum computers and based on a shared classical/quantum memory model [38]. By using this instruction we implement the Eq.(9) on pyQuil by below code:

```

from pyquil.quil import
from pyquil.api import WavefunctionSimulator
for i in list1:
p+=H(i),CPHASE(np.pi,i+1,i),RX(0.25,i),CPHASE(np.pi,i+1,i),H(i),RZ(0.25,i)
for i in list1:
if i>0:
p+=X(i)
p+=X(2),X(4),X(6)
for i in list1:
p+=H(i),CPHASE(np.pi,i+1,i),RX(0.25,i),CPHASE(np.pi,i+1,i),H(i),RZ(0.25,i)
for i in list1:
if i>0:
p+=X(i)
for i in list1:
p+=H(i),CPHASE(np.pi,i+1,i),RX(0.25,i),CPHASE(np.pi,i+1,i),H(i),RZ(0.25,i)
p+=X(2),X(4),X(6) # # # #

```

Similarly, the code to implement of Ee.(15) can be written straightforward.

### Appendix II

To solve the master equation which  $\mathcal{L}$  is the generator of a semigroup of a quantum channel at first we must find left and right eigen-operators  $L_k$  and  $R_k$  which satisfying the following condition:

$$L_k \mathcal{L} = \lambda_{(k,j)} L_k, \quad (31)$$

$$R_k \mathcal{L} = \lambda_{(k,j)} R_k, \quad (32)$$

By using the left action of super-operator that defined as  $tr[(\ell(\rho))O] = tr[(O\ell)\rho]$  for arbitrary Hermitian operator  $O$  and any density matrix can find that

$tr[L_k R_m] = \delta_{km}$  and  $\lambda_{(L,k)} = \lambda_{(R,k)}$  where  $tr$  refers to the usual trace, so that initial state writing in damping base method such [40, 41]

$$\rho(0) = \sum_k tr[L_k \rho(0)] R_k, \quad (33)$$

and

$$\rho(t) = e^{\mathcal{L}t}[\rho(0)] = \sum_k tr[L_k \rho(0)] \Lambda_k R_k, \quad (34)$$

where  $\Lambda_k = e^{\lambda_k t}$ . So for solving equation (23) we utilize these set  $\{I, \sigma_z, \sigma^+$  and  $\sigma^-\}$  as right eigen-operators, we obtain:

$$\mathcal{L}_R(I) = -8\Gamma\sigma_z, \quad (35)$$

$$\mathcal{L}_R(\sigma_z) = -8\Gamma\sigma_z, \quad (36)$$

$$\mathcal{L}_R(\sigma^+) = -4\Gamma\sigma^+, \quad (37)$$

$$\mathcal{L}_R(\sigma^-) = -4\Gamma\sigma^-, \quad (38)$$

For left eigen-operators action we consider an appropriate set of operators  $\{I - \sigma_z, \sigma_z, \sigma^+$  and  $\sigma^-\}$

$$\mathcal{L}_L(I - \sigma_z) = 0, \quad (39)$$

$$\mathcal{L}_L(\sigma_z) = -8\Gamma\sigma_z, \quad (40)$$

$$\mathcal{L}_L(\sigma^+) = -4\Gamma\sigma^+, \quad (41)$$

$$\mathcal{L}_L(\sigma^-) = -4\Gamma\sigma^-, \quad (42)$$

so  $tr[L_1 \rho(0)] = 1/2(1-r_z)$ ,  $tr[L_2 \rho(0)] = 1/2r_z$ ,  $tr[L_3 \rho(0)] = 1/4(r_x + ir_y)$  and  $tr[L_4 \rho(0)] = 1/4(r_x - ir_y)$  and using Eq.(34) we can easily obtain Eq.(24).

## References

- [1] R. P. Feynman, "Simulating physics with computers," *Int. J. Theor. Phys.*, vol. 21, no. 6-7, pp. 467–488, 1982.
- [2] D. Porras and J. I. Cirac, "Effective quantum spin systems with trapped ions," *Phys. Rev. Lett.*, vol. 92, no. 20, p. 207901, 2004.

- [3] K. Kim, M.-S. Chang, S. Korenblit, R. Islam, E. E. Edwards, J. K. Freericks, G.-D. Lin, L.-M. Duan, and C. Monroe, “Quantum simulation of frustrated ising spins with trapped ions,” *Nature*, vol. 465, no. 7298, p. 590, 2010.
- [4] D. Jaksch and P. Zoller, “The cold atom hubbard toolbox,” *Annals of physics*, vol. 315, no. 1, pp. 52–79, 2005.
- [5] J. You and F. Nori, “Atomic physics and quantum optics using superconducting circuits,” *Nature*, vol. 474, no. 7353, p. 589, 2011.
- [6] J. Clarke and F. K. Wilhelm, “Superconducting quantum bits,” *Nature*, vol. 453, no. 7198, p. 1031, 2008.
- [7] J. Cho, D. G. Angelakis, and S. Bose, “Fractional quantum hall state in coupled cavities,” *Phys. Rev. Lett.*, vol. 101, no. 24, p. 246809, 2008.
- [8] E. Manousakis, “A quantum-dot array as model for copper-oxide superconductors: A dedicated quantum simulator for the many-fermion problem,” *J. Low Temp. Phys.*, vol. 126, no. 5-6, pp. 1501–1513, 2002.
- [9] A. F. Fahmy and T. F. Havel, “Nuclear magnetic resonance spectroscopy: An experimentally accessible paradigm for quantum computing,” *Quantum Computation and Quantum Information Theory: Reprint Volume with Introductory Notes for ISI TMR Network School, 12-23 July 1999, Villa Gualino, Torino, Italy*, p. 471, 2000.
- [10] N. A. Gershenfeld and I. L. Chuang, “Bulk spin-resonance quantum computation,” *science*, vol. 275, no. 5298, pp. 350–356, 1997.
- [11] D. G. Cory, A. F. Fahmy, and T. F. Havel, “Ensemble quantum computing by nmr spectroscopy,” *Proc. Nat. Acad. Sci.*, vol. 94, no. 5, pp. 1634–1639, 1997.
- [12] Z. Li, M.-H. Yung, H. Chen, D. Lu, J. D. Whitfield, X. Peng, A. Aspuru-Guzik, and J. Du, “Solving quantum ground-state problems with nuclear magnetic resonance,” *Scientific reports*, vol. 1, p. 88, 2011.
- [13] J. Zhang, M.-H. Yung, R. Laflamme, A. Aspuru-Guzik, and J. Baugh, “Digital quantum simulation of the statistical mechanics of a frustrated magnet,” *Nature Communications*, vol. 3, p. 880, 2012.



- [14] H.-P. Breuer, F. Petruccione, *et al.*, *The theory of open quantum systems*. Oxford University Press on Demand, 2002.
- [15] M. Hillery, M. Ziman, and V. Bužek, “Implementation of quantum maps by programmable quantum processors,” *Phys. Rev. A*, vol. 66, no. 4, p. 042302, 2002.
- [16] D. Bacon, A. M. Childs, I. L. Chuang, J. Kempe, D. W. Leung, and X. Zhou, “Universal simulation of markovian quantum dynamics,” *Phys. Rev. A*, vol. 64, no. 6, p. 062302, 2001.
- [17] M. Ziman, P. Štelmachovič, and V. Bužek, “Description of quantum dynamics of open systems based on collision-like models,” *J. Open Syst. Inform. Dynam.*, vol. 12, no. 1, pp. 81–91, 2005.
- [18] M. Koniorczyk, V. Buzek, P. Adam, and A. Laszlo, “Simulation of markovian quantum dynamics on quantum logic networks,” *arXiv preprint quant-ph/0205008*, 2002.
- [19] M. Koniorczyk, V. Bužek, and P. Adam, “Simulation of generators of markovian dynamics on programmable quantum processors,” *J. Eur. Phys. D*, vol. 37, no. 2, pp. 275–281, 2006.
- [20] D.-S. Wang, D. W. Berry, M. C. de Oliveira, and B. C. Sanders, “Solovay-kitaev decomposition strategy for single-qubit channels,” *Phys. Rev. Lett.*, vol. 111, no. 13, p. 130504, 2013.
- [21] N. Lambert, Y.-N. Chen, Y.-C. Cheng, C.-M. Li, G.-Y. Chen, and F. Nori, “Quantum biology,” *Nature Physics*, vol. 9, no. 1, p. 10, 2013.
- [22] A. Chin, S. Huelga, and M. Plenio, “Coherence and decoherence in biological systems: principles of noise-assisted transport and the origin of long-lived coherences,” *Phil. Trans. R. Soc. A*, vol. 370, no. 1972, pp. 3638–3657, 2012.
- [23] O. Sinanoğlu, *Modern Quantum Chemistry: Action of light and organic crystals*. Academic Press, 1965.
- [24] M. Grover and R. Silbey, “Exciton migration in molecular crystals,” *J. Chem. Phys.*, vol. 54, no. 11, pp. 4843–4851, 1971.

- [25] M. Yang and G. R. Fleming, “Influence of phonons on exciton transfer dynamics: comparison of the redfield, förster, and modified redfield equations,” *J. Chem. Phys.*, vol. 282, no. 1, pp. 163–180, 2002.
- [26] V. I. Novoderezhkin, M. A. Palacios, H. Van Amerongen, and R. Van Grondelle, “Energy-transfer dynamics in the lhci complex of higher plants: modified redfield approach,” *J. Phys. Chem. B*, vol. 108, no. 29, pp. 10363–10375, 2004.
- [27] S. Jang, M. D. Newton, and R. J. Silbey, “Multichromophoric förster resonance energy transfer,” *Phys. Rev. Lett.*, vol. 92, no. 21, p. 218301, 2004.
- [28] V. V. Poddubnyy, I. O. Glebov, and V. V. Eremin, “Non-markov dissipative dynamics of electron transfer in a photosynthetic reaction center,” *Theoretical and Mathematical Physics*, vol. 178, no. 2, pp. 257–264, 2014.
- [29] F. Caruso, A. W. Chin, A. Datta, S. F. Huelga, and M. B. Plenio, “Entanglement and entangling power of the dynamics in light-harvesting complexes,” *Phys. Rev. A*, vol. 81, no. 6, p. 062346, 2010.
- [30] X. Wang, G. Ritschel, S. Wüster, and A. Eisfeld, “Open quantum system parameters for light harvesting complexes from molecular dynamics,” *J. Physical Chemistry Chemical Physics (PCCP)*, vol. 17, no. 38, pp. 25629–25641, 2015.
- [31] F. Caruso, A. W. Chin, A. Datta, S. F. Huelga, and M. B. Plenio, “Highly efficient energy excitation transfer in light-harvesting complexes: The fundamental role of noise-assisted transport,” *J. Chem. Phys.*, vol. 131, no. 10, p. 09B612, 2009.
- [32] J. Moix, J. Wu, P. Huo, D. Coker, and J. Cao, “Efficient energy transfer in light-harvesting systems, iii: The influence of the eighth bacteriochlorophyll on the dynamics and efficiency in fmo,” *The Journal of Physical Chemistry Letters*, vol. 2, no. 24, pp. 3045–3052, 2011.
- [33] S.-H. Yeh and S. Kais, “Simulated two-dimensional electronic spectroscopy of the eight-bacteriochlorophyll fmo complex,” *J. Phys. Chem.*, vol. 141, no. 23, p. 12B645\_1, 2014.

- [34] S. Mostame, J. Huh, C. Kreisbeck, A. J. Kerman, T. Fujita, A. Eisfeld, and A. Aspuru-Guzik, “Emulation of complex open quantum systems using superconducting qubits,” *J. Quantum Inf. Process.*, vol. 16, no. 2, p. 44, 2017.
- [35] A. Chin, J. Prior, R. Rosenbach, F. Caycedo-Soler, S. Huelga, and M. Plenio, “The role of non-equilibrium vibrational structures in electronic coherence and recoherence in pigment–protein complexes,” *Nature Physics*, vol. 9, no. 2, p. 113, 2013.
- [36] D. W. Leung, I. L. Chuang, F. Yamaguchi, and Y. Yamamoto, “Efficient implementation of coupled logic gates for quantum computation,” *Phys. Rev. A*, vol. 61, no. 4, p. 042310, 2000.
- [37] H. F. Trotter, “On the product of semi-groups of operators,” *Proc. Am. Math. Soc.*, vol. 10, no. 4, pp. 545–551, 1959.
- [38] R. S. Smith, M. J. Curtis, and W. J. Zeng, “A practical quantum instruction set architecture,” *arXiv preprint arXiv:1608.03355*, 2016.
- [39] M. B. Ruskai, S. Szarek, and E. Werner, “An analysis of completely-positive trace-preserving maps on 2x2 matrices,” *arXiv preprint quant-ph/0101003*, 2000.
- [40] S. Daffer, K. Wódkiewicz, and J. K. McIver, “Quantum markov channels for qubits,” *Phys. Rev. A*, vol. 67, no. 6, p. 062312, 2003.
- [41] H.-J. Briegel and B.-G. Englert, “Quantum optical master equations: The use of damping bases,” *Phys. Rev. A*, vol. 47, no. 4, p. 3311, 1993.
- [42] C. P. Slichter, *Principles of magnetic resonance*, vol. 1. Springer Science & Business Media, 2013.